ChemComm

Isoacenofuran: novel quinoidal building block for efficient access to high-ordered polyacene derivatives

Journal:	*ChemComm*
Manuscript ID	CC-COM-10-2020-006620.R1
Article Type:	Communication

Journal Name

COMMUNICATION

Isoacenofuran: novel quinoidal building block for efficient access to high-ordered polyacene derivatives

Received 00th January 20xx,
Accepted 00th January 20xx

DOI: 10.1039/x0xx00000x

www.rsc.org/

Kei Kitamura,[a,b] Ryoji Kudo,[a] Haruki Sugiyama,[c] Hidehiro Uekusa,[c] and Toshiyuki Hamura*[a]

Herein, a simple and practical method for generating isoacenofuran, a new π-extended quinoidal building block, was developed. A three-step protocol involving double nucleophilic additions of alkynyllithiums to acene-2,3-dicarbaldehyde, mono-oxidation, and acid-promoted cyclization enables the generation of the target molecule, which is trapped by a dienophile to produce highly condensed acenequinones. Further transformations by double nucleophilic additions of alkynyllithium to hexacenequinone, followed by reductive aromatization, produce tetraalkynylhexacenes with remarkably higher stability than previously reported substituted hexacenes.

Isoacenofuran (aceno[2,3-c]furan) is a novel class of heteroacene in which the *o*-quinoidal structure is only drawn in the closed-shell resonance form. Therefore, it possesses various unique physical properties compared to analogous isoelectronic acene (aceno[2,3-b]furan).[1–3] Linearly fused π-extended homologs, e.g., isonaphthofuran and isoanthracenofuran, have higher reactivity than the parent isobenzofuran; hence, they can serve as reactive platforms for the rapid construction of high-ordered polycyclic systems. However, methods for the synthesis of π-extended homologs are limited because their instability increases with the presence of more quinoidal groups.[4]

In this context, we previously reported the preparation of diarylisoanthracenofuran **4** through the [4+2] cycloaddition of didehydroisobenzofuran **1** and isobenzofuran **2**, followed by the reductive aromatization of the resulting polycycle **3**.[5] However, this method has a drawback in that steric protection around the furan moiety is required to suppress the competing cycloaddition from the initially formed cycloadduct **3**. In contrast, the double nucleophilic addition of alkynyllithium to acene-2,3-carbaldehyde **5** and acid-promoted cyclization effectively generate dialkynylisoacenofurans **7–9**. Importantly, π-extended isobenzofurans generated via this method were trapped with dienophiles to produce polyaceneqinones having various synthetic potentials. Moreover, tetrakis-(arylethynyl)hexacene, a high-order acene with very few synthetic examples, could be prepared by this strategy,[6,7] and its structure was characterized by X-ray crystal structure analysis, which are described in this communication.

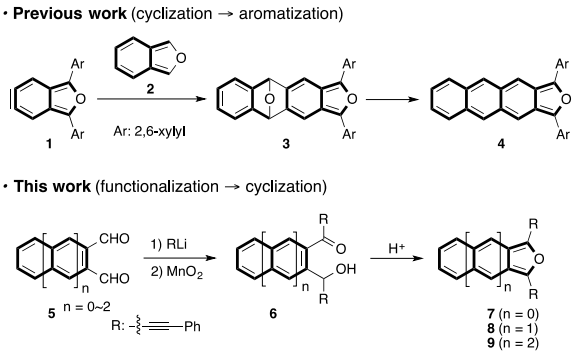

Scheme 1 Isoacenofuran, a novel class of heteroacene with potentially high reactivity.

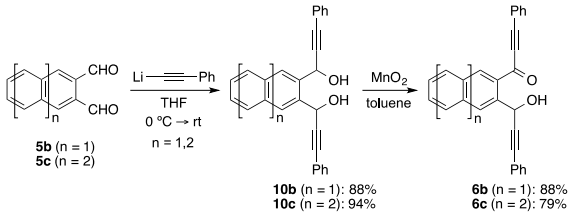

Scheme 2 Synthesis of the of keto-alcohols **6b** and **6c**.

Scheme 2 shows the preparation of keto-alcohol **6**, a precursor of isoacenofuran. Upon treatment of 2,3-

[a] *Department of Applied Chemistry for Environment, School of Science and Technology, Kwansei Gakuin University, 2-1 Gakuen, Sanda, Hyogo 669-1337, Japan. E-mail: thamura@kwansei.ac.jp*
[b] *Present address: Faculty of Pharmaceutical Sciences, Tokushima Bunri University, 180 Yamashiro-cho, Tokushima 770-8514, Japan.*
[c] *Department of Chemistry, School of Science, Tokyo Institute of Technology, Ookayama 2, Meguro-ku, Tokyo 152-8551, Japan*
† Footnotes relating to the title and/or authors should appear here.
Electronic Supplementary Information (ESI) available: [details of any supplementary information available should be included here]. See DOI: 10.1039/x0xx00000x

naphthalenedicarbaldehyde **5b** with phenylethynyllithium (THF, 0 °C → r.t.), double nucleophilic additions afforded diol **10b** as a mixture of diastereomers. Subsequent mono-oxidation of diol **10b** with MnO_2 produced keto-alcohol **6b**. In a similar fashion, condensed keto-alcohol **6c** was prepared from 2,3-anthracenedicarbaldehyde **5c**.

Scheme 3 shows the preparation of isonaphthofuran **8**. Based on our previously developed synthetic method for 1,3-bis(phenylethynyl)isobenzofuran (**7**),[3b,3c] keto-alcohol **6b** was treated with 4 M HCl (0 °C → r.t.). In this case, however, the starting material (**6b**) was not consumed at all at this temperature, suggesting that the formation rate of isonaphthofuran **8** is lower than that of isobenzofuran **7**. TLC analysis showed that isonaphthofuran **8** was formed at a higher reaction temperature (40 °C). Unfortunately, however, isolation using the conventional method was unsuccessful due to the higher reactivity of **8**, resulting in its decomposition during purification.

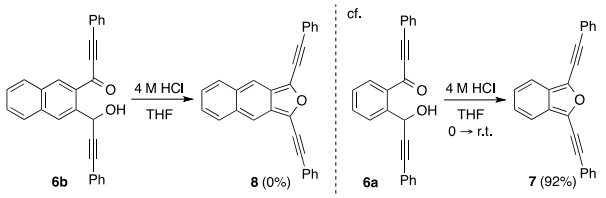

Scheme 3 Unsuccessful attempt on preparation of isoacenofuran **8**.

Further examination revealed that isonaphthofuran **8** could be trapped under suitable conditions (Table 1). Upon treatment of keto-alcohol **6a** with 4 M HCl in the presence of naphthoquinone **11** (r.t. → 40 °C), [4+2] cycloaddition afforded cycloadduct **14** in 32% yield as a mixture of stereoisomers (entry 1). The stereochemistry of the product was tentatively assigned by considering the chemical shift of each methine proton (endo-**14**/exo-**14** = 74/26).[8] Further screening of the reaction conditions indicated that TFA was more effective in generating isonaphthofuran **8**, producing cycloadduct **14** in 86% yield (entry 2).

Table 1 Generation and trapping of isonaphthofuran **8**.

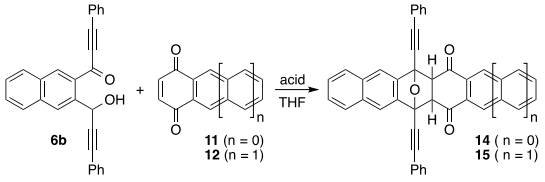

Entry	Acid [a]	Conditions	Yield/%
1	4 M HCl	0 °C → r.t.	**14**: 0 [b]
2	4 M HCl	r.t. → 40 °C	**14**: 32
3	CF_3CO_2H	r.t.	**14**: 86
4	CF_3CO_2H	r.t.	**15**: 94 [c]

[a]Acid (2.5 equiv) was used. [b]The starting material was recovered. [c]Endo-**15**/exo-**15** = 93/7.

Importantly, cycloadduct **14** was thermodynamically stable, in sharp contrast to cycloadduct **13** (structure, see Table 2) obtained through the reaction of isobenzofuran **7** and **11**,[9] which underwent rapid retro Diels–Alder reaction in solution (*vide infra*). As the trapping agent, anthraquinone **12** worked well, and cyclization with isonaphthofuran **8** produced a heptacyclic compound **15** in excellent yield (entry 3).

Next, we verified the possibility of generating isoanthracenofuran **9**, a higher homolog of isoacenofuran (Scheme 4). Due to the greater loss of aromatic character by the formation of acenofuran with further π-extension, a higher reaction temperature (60 °C) was required to form isoanthracenofuran **9**, which, in turn, was cyclized with trapping agents **11** or **12**, creating cycloadducts **16** and **17** in 89% and 78% yields, respectively. The conversion of [4+2] cycloadduct **17** to heptacenequinone **18**, a useful building block for further functionalization, was performed under basic conditions (DBU, LiI, CH_2Cl_2, 0 °C).

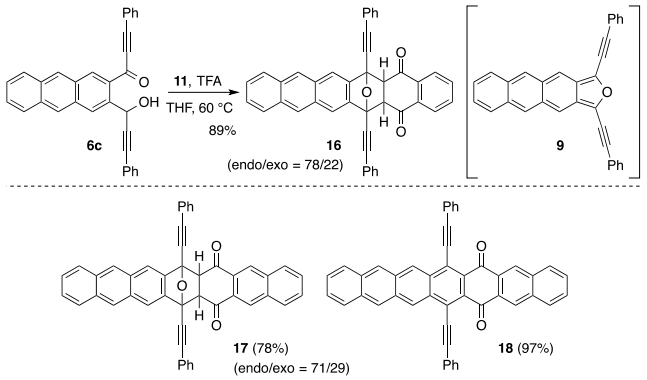

Scheme 4 Generation and trapping of isoanthracenofuran **9**.

We performed theoretical calculations to evaluate the energy changes resulting from the cycloadditions of isoacenofurans **7**–**9** and naphthoquinone (**11**) (Table 2). The data indicated that the reaction of isobenzofuran **7** with **11** was endothermic and that the formation of cycloadduct **13**-**endo** was thermodynamically disfavored by 2.2 kcal/mol. Indeed, the cycloreversion of the cycloadduct **13**-**endo** to isobenzofuran **7** occurred at room temperature in $CDCl_3$, which was monitored by ^1H NMR (Figure S10).[10,11]

Table 2 Energy change resulting from the cycloaddition of isoacenofuran and frontier orbital levels of isoacenofuran.

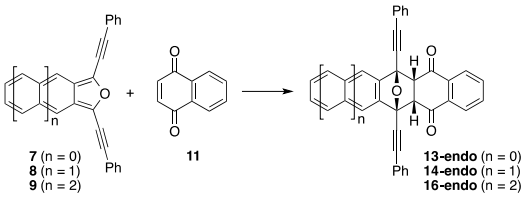

furan	ΔE (kcal/mol)[b]	HOMO (eV)	LUMO (eV)
7	+2.2	−4.82	−2.08
8	−4.2	−4.59	−2.38

9	−7.0	−4.42	−2.62

[a]The calculations were carried out at the B3LYP/6-31G* level. [b]$\Delta E = E_{cycloadduct} - E_{isoacenofuran} - E_{naphthoquinone}$.

In contrast, the corresponding reactions of isoacenofurans **8** and **9** were exothermic. Among these, cycloadduct **16**-**endo** was the most thermodynamically favored ($\Delta E = -7.0$ kcal/mol). This tendency can be explained by the reactivity order of isoacenofurans, **9** > **8** > **7**, which is closely correlated with the smaller HOMO–LUMO gap of isoacenofurans, showing the more butadiene character (less aromatic character). The highest energy level of the HOMO of **9** also explains the high reactivity. Based on these results, we expect that, compared to lower homologs, higher furan homologs will form more slowly although they will react more quickly.

Furthermore, we examined the syntheses of substituted hexacenes possessing multiple alkynyl groups on the periphery by considering highly condensed polyacenequinones with greater-than-pentacene structures.[6] According to our previous report on tetrakis(phenylethynyl)tetracene (**23**),[7d] hexacenequinone **19**, prepared by the base-promoted aromatization of cycloadduct **15**, was converted to 6,7,14,15-tetrakis(phenylethynyl)hexacene (**21**) via the double nucleophilic additions of phenylethynyllithium to **19**, followed by the reductive aromatization of the resulting diol **20** ($SnCl_2$, conc. HCl, DMF). Importantly, **21** was stable enough to remain in its solid state for several months. ^{1}H NMR analysis revealed that hexacene **21** in $CDCl_3$ gradually decomposed to unidentified products (Figure S11).[12] Similarly, sterically congested hexacene **22** was synthesized to give 42% overall yield by using bis-2,4,6-mesitylethynyl-isonaphthofuran as a reactive building block.[13] It is notable that the solubility of **22** was drastically increased by introducing sterically crowded alkynyl groups to the hexacene core (2 mg/mL, $CHCl_3$). Remarkably, this showed high stability (vide infra).

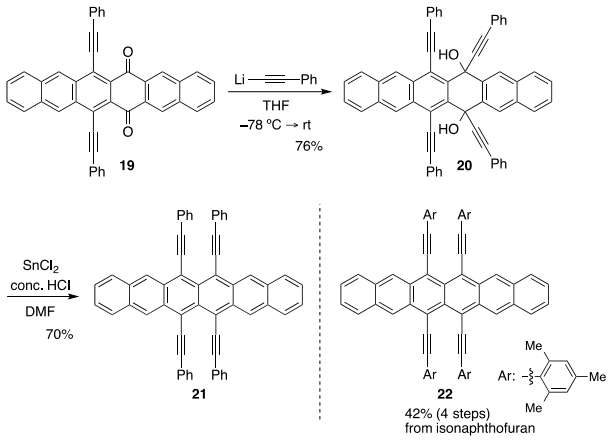

Scheme 5 Preparation of substituted hexacenes **21** and **22**.

The structure of tetraalkynylhexacene **22** was elucidated by X-ray crystal structure analysis (Figures 1).[14] One distinctive feature of **22** is that it adopts a planar conformation in its hexacene core (the end-to-end twist of the hexacene core is 0°). Furthermore, it has a highly distorted structure, avoiding the intramolecular steric repulsion of the *peri*-arylethynyl groups. The distance between the substituents at the *peri*-position of the hexacene plane is extended by expanding the relevant bond angles of hexacene (C_{11}-C_{12}-C_{13} = 122.3°). The arylethynyl groups are arranged one above the other from the hexacene plane, forming a dihedral angle of 26.1°. In addition, the sp carbon atoms of the acetylene units are deformed from linearity (e.g., C_{11}-C_{14}-C_{15} = 174.9°, C_{14}-C_{15}-C_{16} = 170.2°). Moreover, the arylethynyl groups are rotated out of the hexacene plane, in which the proximal aromatic groups bound to the *sp*-hybridized carbons are parallel to each other, thus avoiding steric repulsion. Regarding the crystal packing arrangement, **22** exhibited a one-dimensional π-stacking motif, with a close contact of 3.51 Å between the aromatic faces.

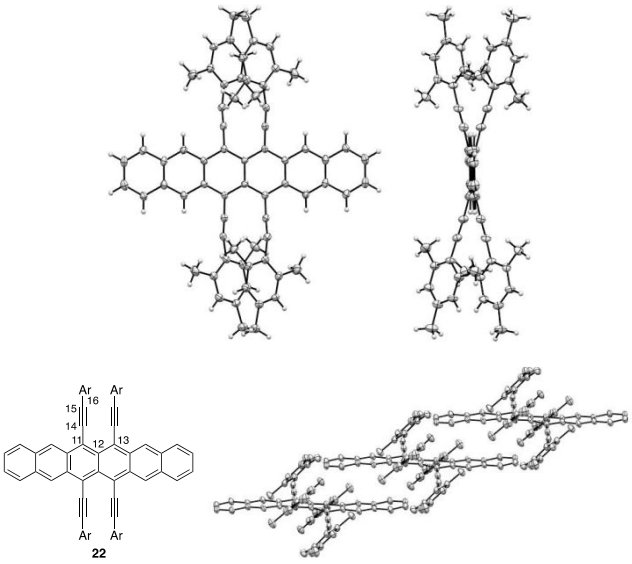

Figure 1 X-ray crystal structure of **22** (upper left: top view, upper right: side view, lower right: crystal packing arrangement; hydrogen atoms are omitted for clarity.). Displacement ellipsoids are drawn at the 50% probability level.

The absorption spectra of hexacene **21** in $CHCl_3$, shown in Figure 2, are compared with those of tetracene **23**. While tetracene **23** has its absorption maximum at 640 nm, the absorption of hexacene **21** peaks at 845 nm and tails up to 980 nm, which is a near infrared region. Thus, from these results, we can conclude that the introduction of two additional aromatic rings to tetracene **23** exerts an effective π-extension, leading to a red-shift of the absorption maximum at approximately 200 nm.

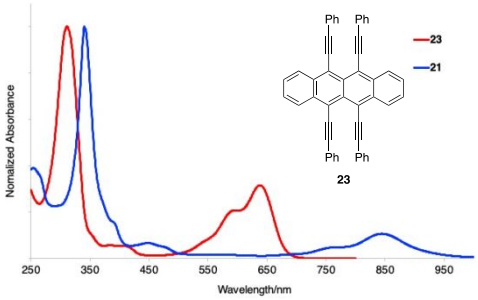

Figure 2 UV-vis-NIR absorption spectra of tetracene **23** and hexacene **21** (in $CHCl_3$).

Furthermore, the half-life of hexacene **21** was estimated to be ~17 h under ambient conditions (Figure S5). Moreover, the sterically crowded hexacene **22** exhibits an absorption maximum at 853 nm (Figure S6), which is slightly red-shifted by ~8 nm compared to that of hexacene **21**. Importantly, this represents markedly enhanced stability toward light and/or air, as evidenced by the half-life of 99 h (Figure S7). To the best of our knowledge, hexacene **22** is the most stable compound among the previously reported substituted hexacenes.[15]

Next, the electrochemical properties of these novel π-conjugated molecules were studied through cyclic voltammetry; the data are summarized in Table S1. The cyclic voltammogram of tetracene **23** shows two reversible reduction waves ($E_{1/2}$ = –1.33, –1.73 V) and a single oxidation wave ($E_{1/2}$ = +0.60 V, Figure S8). Unfortunately, however, hexacene **21** could not be analyzed because of its instability under the measurement conditions. Instead, the more stable hexacene **22** was measured (Figure S9), showing two reversible reduction waves ($E_{1/2}$ = –1.18, 1.46 V) and a single oxidation wave ($E_{1/2}$ = +0.21 V). The electrochemically derived energy band gap of **22** was 1.39 V, which is in good agreement with that obtained from the onset of the absorption spectra (948 nm, 1.31 V). DFT calculations (B3LYP/6-311G**) also supported the HOMO–LUMO gap (1.34 V). Notably, the E_{red1} of **22** was positively shifted by 0.15 V compared to that of tetracene **23**, indicating that it possessed low lying LUMO energy (–3.62 eV). This is due to the existence of multiple alkynyl groups on the hexacene core, which would retard photooxidation and/or photodimerization due to their steric and electronic features.[16] Herein, we propose an efficient method for the synthesis of dialkynylisoacenofuran. This reactive intermediate could serve as a new quinoidal building block to prepare high-ordered polyacene derivatives. Importantly, the introduction of multiple alkynyl groups onto the hexacene core contributed to the high stability of the product, which is an important finding for the future design of stable acene-based materials.

Acknowledgement

This work was supported by JSPS KAKENHI Grant Number JP15H05840 in Middle Molecular Strategy and JST ACT-C Grant Number JPMJCR12YY, Japan.

Conflicts of interest

There are no conflicts to declare.

Notes and references

1 For selected reviews on isobenzofurans: (a) W. Friedrichsen, *Adv. Heterocyl. Chem.,* 1980, **26**, 135–241; (b) W. Friedrichsen, *Adv. Heterocyl. Chem.,* 1999, **73**, 1–96; (c) B. Rickborn, *Advances in Theoretically Interesting Molecules*; Thummel, R. P., Ed.; JAI: Greenwich, Connecticut, 1989, Vol. 1, pp. 1–69.

2 For selective synthetic examples of isobenzofuans, see: (a) P. Binger, P. Wedemann, R. Goddard and U. H. Brinker, *J. Org. Chem*., 1996, **61**, 6462–6464; (b) S.-H. Chan, C.-Y. Yick and H. N. C. Wong, *Tetrahedron,* 2002, **58**, 9413–9422; (c) J. E. Rainbolt and G. P. Miller, *J. Org. Chem.,* 2007, **72**, 3020–3030.

3 For our developed synthetic methods for functionalized isobenzofurans: (a) T. Hamura and R. Nakayama, *Chem. Lett*., 2013, **42**, 1013–1015; (b) K. Asahina, S. Matsuoka, R. Nakayama and T. Hamura, *Org. Biomol. Chem*., 2014, **12**, 9773–9776; (c) R. Kudo, K. Kitamura and T. Hamura, *Chem. Lett*., 2017, **46**, 25–28.

4 (a) M. P. Cava and J. P. VanMeter, *J. Org. Chem*., 1969, **34**, 538–545; (b) K.-D. Gundermann, M. Steinfatt, P. Witt, C. Paetz and K.-L. Poeppel, *J. Chem. Res. (M)*, 1980, 2801–2822; (c) W. C. Christopfel and L. L. Miller, *J. Org. Chem*., 1986, **51**, 4169–4175; (d) N. P. W. Tu, J. C. Yip and P. W. Dibble, *Synthesis*, 1996, **01**, 77–81; (e) R. Mondal, B. K. Shah and D. C. Neckers, *J. Org. Chem*., 2006, **71**, 4085–4091; (f) J. Lu, D. M. Ho, N. J. Vogelaar, C. M. Kraml, S. Bernhard, N. Byrne, L. R. Kim and R. A. Pascal, Jr. *J. Am. Chem. Soc*., 2006, **128**, 17043–17050.

5 S. Matsuoka, S. Jung, K. Miyakawa, Y. Chuda, R. Sugimoto and T. Hamura, *Chem. – Eur. J*., 2018, **24**, 18886–18889.

6 For selected reviews on polyacenes, see: (a) M. Bendikov, F. Wudl and D. F. Perepichka, *Chem. Rev*., 2004, **104**, 4891–4946; (b) J. E. Anthony, *Angew. Chem. Int. Ed*., 2008, **47**, 452–483; (c) H. F. Bettinger, *Pure Appl. Chem*., 2010, **82**, 905–915.

7 For our synthetic application of isobenzofurans to polyacene derivatives, see: (a) H. Haneda, S. Eda, M. Aratani and T. Hamura, *Org. Lett.,* 2014, **16**, 286–289; (b) R. Akita, K. Kawanishi and T. Hamura, *Org. Lett.,* 2015, **17**, 3094–3097; (c) S. Eda, F. Eguchi, H. Haneda and T. Hamura, *Chem. Commun.,* 2015, **51**, 5963–5966; (d) K. Kitamura, K. Asahina, Y. Nagai, H. Sugiyama, H. Uekusa and T. Hamura, *Chem. – Eur. J*., 2018, **24**, 14034–14038; (e) K. Kitamura, K. Asahina, Y. Nagai, Z. Keshu, S. Nomura, K. Tanaka and T. Hamura, *Org. Biomol. Chem*., 2018, **16**, 9143–9146.

8 For related [4+2] cycloaddition of diphenylisobenzofuran with 1,4-naphthoquinone and structural characterization of the endo/exo-cycloadducts, see: T. Wombacher, S. Foro and J. J. Schneider, *Eur. J. Org. Chem.,* 2016, **3**, 569–578. See also ref. 7b. For details, see the supporting information.

9 The solvent choice was important to obtain cycloadduct **13**, which was precipitated from the solvent. For details, see ref. 7e.

10 For details, see supporting information. See also ref. 7e.

11 For related cycloreversion of the isobenzofuran-naphthoquinone cycloadduct, please refer to: J. A. Dodge, J. D. Bain and A. R. Chamberlin, *J. Org. Chem.,* 1990, **55**, 4190–4198. See also ref. 8.

12 Due to the low solubility of hexacene **21** in common organic solvents, ^{13}C NMR spectra of **21** could not be obtained.

13 For preparation of hexacene **22**, see supporting information.

14 Crystal data for **22**: $C_{70}H_{56}$, MW = 897.14, 0.180 × 0.028 × 0.028 mm, Monoclinic, space group $P\,2_1/n$, Z =2, T = 93(2) K, a = 8.80384(16) Å, b = 9.18711(17) Å, c = 30.3074(6) Å, α = 90°, β = 96.5951(10)°, γ = 90°, V = 2435.10(8) Å^3, λ(Cu Kα) = 1.54186 Å, μ = 0.520 mm^{-1}. Intensity data were collected on Rigaku R-AXIS RAPID II. The structure was solved by direct methods (*SHELXT 2014/4*) and refined by the full-matrix least-squares method *on* F^2 (*SHELXL*-2018/1). A total of 52552 reflections were measured and 52552 were independent. Final R_1 = 0.0887, wR_2 = 0.2264 (24533 refs; $I > 2\sigma(I)$), and GOF = 0.994 (for all data, R_1 = 0.1527, wR_2 = 0.2787).

15 (a) M. M. Payne, S. R. Parkin and J. E. Anthony, *J. Am. Chem. Soc*., 2005, **127**, 8028–8029; (b) B. Purushothaman, S. R. Parkin and J. E. Anthony, *Org. Lett*., 2010, **12**, 2060–2063; (c) R. Mondal, R. M. Adhikari, B. K. Shah and D. C. Neckers, *Org. Lett*., 2007, **9**, 2505–2508.

16 W. Fudickar and T. Linker, *J. Am. Chem. Soc*., 2012, **134**, 15071–15082.